Available online at BCREC Website: http://bcrec.undip.ac.id

Bulletin of Chemical Reaction Engineering & Catalysis, 11 (1), 2016, 10-20

Research Article

Electro-oxidation of Ethanol on Carbon Supported PtSn and PtSnNi Catalysts

Nur Hidayati[1]*, Keith Scott[2]

[1]*Department of Chemical Engineering, Universitas Muhammadiyah Surakarta*
Jl. A. Yani Tromol Pos 1 Pabelan Kartasura, Surakarta, Indonesia
[2]*School of Chemical Engineering and Advanced Materials, Newcastle University*
Newcastle upon Tyne, NE1 7RU, UK

Received: 10th November 2015; Revised: 1st February 2016; Accepted: 1st February 2016

Abstract

Even though platinum is known as an active electro-catalyst for ethanol oxidation at low temperatures (< 100 °C), choosing the electrode material for ethanol electro-oxidation is a crucial issue. It is due to its property which easily poisoned by a strong adsorbed species such as CO. PtSn-based electro-catalysts have been identified as better catalysts for ethanol electro-oxidation. The third material is supposed to improve binary catalysts performance. This work presents a study of the ethanol electro-oxidation on carbon supported Pt-Sn and Pt-Sn-Ni catalysts. These catalysts were prepared by alcohol reduction. Nano-particles with diameters between 2.5-5.0 nm were obtained. The peak of (220) crystalline face centred cubic (fcc) Pt phase for PtSn and PtSnNi alloys was repositioned due to the presence of Sn and/or Ni in the alloy. Furthermore, the modification of Pt with Sn and SnNi improved ethanol and CO electro-oxidation.

Keywords: Direct Ethanol Fuel Cells; ethanol electro-oxidation catalysts; PtSn/C; PtSnNi/C

How to Cite: Hidayati, N., Scott, K. (2016). Electro-oxidation of Ethanol on Carbon Supported PtSn and PtSnNi Catalysts. *Bulletin of Chemical Reaction Engineering & Catalysis*, 11 (1): 10-20. (doi:10.9767/bcrec.11.1.399.10-20)

Permalink/DOI: http://dx.doi.org/10.9767/bcrec.11.1.399.10-20

1. Introduction

It is well known that Pt is a good electro-catalyst for oxidation but does not exhibit high activity for ethanol electro-oxidation [1, 2]. Research has thus focused on the use of alloy catalysts to improve the electro-activity of Pt [3-8]. Metals such as Sn have been identified as suitable materials to form alloys with Pt for ethanol electro-oxidation in acid solutions [8–10]. However, the performance of PtSn/C catalyst depends on the preparation procedures, the Pt:Sn atomic ratio and catalyst structure [2, 11-15]. Zhou *et al*. [16] observed that the optimum Sn content altered the fuel cell maximum density at different temperature.

There are some different preparation methods. Recently, a number of researchers have investigated the ethanol oxidation on carbon supported PtSn catalysts prepared by impregnation reduction method [17], Bonneman's method [13], polyol process [2] and modified borohydride reduction [15]. Nevertheless, the effect of Sn content was not clear. The group of Lamy *et al*., Zhou *et al*., and Kim *et al*. have found the optimum composition of Sn in the range of 10-20 % [13, 17], 33-40 % [2, 18, 19]. and 20-33 % [14], respectively.

* Corresponding Author.
E-mail: nur.hidayati@ums.ac.id (N. Hidayati)

The third material is supposed to improve binary catalysts. Spinace *et al*. [20] have studied the activity of ethanol electro-oxidation on PtSn/C and PtSnNi/C catalysts. It was found that the PtSnNi/C catalyst gives higher current values and superior stability than PtSn/C. However, further investigation is needed in order to find the optimum composition of Pt:Sn:Ni and its application in the DEFCs.

This work presents a study of the ethanol electro-oxidation on carbon supported Pt-Sn and Pt-Sn-Ni catalysts, and their applications as anode catalysts in a single DEFC. These catalysts were prepared by alcohol reduction followed by X-ray diffraction (XRD) and energy dispersive analysis of X-ray (EDAX) characterisations. Electrochemical measurements including linear sweep voltammetry (LSV), chronoamperometry and carbon monoxide stripping voltammetry were also carried out to evaluate the electroactivity of catalysts towards ethanol oxidation.

2. Experimental

2.1. Catalysts Preparation

Carbon supported PtSn with various atomic ratio and PtSnNi catalysts were prepared by the polyol process [2]. $H_2PtCl_6.6H_2O$, $SnCl_2.2H_2O$ and $NiCl_2.6H_2O$ from Aldrich were used as precursors. All samples were supported on Vulcan XC-72R carbon black (Cabot Corp., S_{BET} = 237 m^2 g^{-1}). The precursors were dissolved in ethylene glycol (10% v/v of water) and stirred for 30 minutes. The pH of solution was adjusted between 12 and 13 with sodium hydroxide then heated at temperature of 130 ^oC for about 2 hours to complete the reduction process. The carbon support was mixed with a few drops of ethylene glycol solution and ultrasonicated to form slurry (called as carbon slurry). The carbon slurry was added drop-wise to the metals precursor solution and mixed for about 4 h then cooled down to at room temperature. The solution was filtered, washed and finally dried at 80 ^oC for about 10 h in a vacuum oven.

2.2. Physicochemical Characterisation

Physicochemical characterisation was carried out to obtain information regarding the morphology and structure of the catalysts. Catalyst compositions were confirmed by Energy dispersive X-ray analysis (EDAX) performed using a Rontec attachment, a JEOL 5300LV scanning electron microscope.

Particle sizes were determined by Transmission Electron Microscopy (TEM) using a Philips CM 100 Compustage (FEI) with an AMT CCD camera (Deben). The samples for characterisation were prepared by mixing the catalyst with water and ultrasonicated for a few minutes. A small drop of this mixture containing the catalysts was deposited onto a copper grid covered with a membrane and left to dry. Histograms of particle sizes distribution were constructed using the images obtained from approximately 100 particles. The average particle size of catalysts was calculated from the size distribution.

X-ray diffraction (XRD) was used to analyse the crystallites structure of catalysts. The XRD data were recorded with a PAN analytical X'pert Pro MPD (multipurpose diffractometer) using Cu Kα radiation (l = 1.54056A) and fitted with an X'celerator. Radiation was generated at 40 KV and 40 mA. The 2θ angular regions between 10^o and 90^o were explored at a nominal step size of 0.033^o 2θ and time per step of 100 seconds. The scan was carried out in continuous mode.

2.3. Electrochemical Characterisation

Electrochemical measurements carried out were cyclic voltammetry (CV), linear sweep voltammetry (LSV) and chronoamperometry. Measurements were performed using a PC controlled Voltalab PGZ100 potentiostat, and a conventional three electrode cell. The working electrode was a very thin layer of Nafion® bonded-catalyst deposited on the tip of a glassy carbon rod (BASi MF-2012) with an area of 0.07 cm^2.

The catalyst layer was prepared from a catalyst ink, obtained by ultrasonicating the Pt-based catalyst, 5 wt.% Nafion or PBI solution and ethanol. The solvent was then evaporated in an oven. The quantity of electro-catalysts on the working electrode was 0.005 mg.

The electrochemical tests were performed in a two-compartment glass cell. A lugin capillary probe was fitted to the working electrode chamber for electrode potential measurements and control of potential. The volumes of the cell chambers were 200 cm^3 (mL). A water jacket linked to an external heating bath was employed to perform tests at a controlled temperature. A Pt mesh and an Ag/AgCl electrode were used as the counter and reference electrode, respectively.

Before CV and chronoamperometry measurements, the solution was purged with nitrogen and stirred for twenty minutes to remove oxygen from the solution. The potential was cy-

cled to remove any contaminants at scan rates of 50 mV s^{-1}. CV and LSV data were recorded at a 5 mV s^{-1} scan rate and chronoamperometry was performed at 500 mV.

The CO electro-oxidation was carried out in 0.5 mol dm^{-3} (M) H_2SO_4 solution which was sparged with nitrogen. After a reproducible cyclic voltammogram was obtained, the electrode was held at a potential of 100 mV vs RHE. Meanwhile, carbon monoxide was introduced into the solution for about 15 minutes. Unabsorbed CO was removed by sparging nitrogen into the solution for about 30 minutes. Potentials were then swept at 20 mV s^{-1} and followed by recording the CO stripping voltammogram. All potentials were reported on the standard hydrogen scale.

3. Results and Discussion

EDAX analysis was employed to estimate the nominal composition of the prepared catalysts. The measured Pt:Sn and Pt:Sn:Ni atomic ratios of the prepared catalysts were slightly different from its catalyst solution compositions (Table 1).

Figure 1 shows the typical TEM images and histogram of the particle sizes distribution of PtSn/C and PtSnNi/C catalysts. The particle sizes were found to be in the range of 1 to 10 nm with mean diameters of 3-5 nm. Meanwhile, Figures 2 and 3 show XRD patterns of the carbon supported PtSn and PtSnNi which are compared to the commercial carbon supported Pt (E-TEK), in which the characteristic peak of crystalline face centred cubic (fcc) Pt phase at (111), (200), (220) and (311) planes appear at the corresponding diffraction angles. The diffraction peak at 20-25° observed in all the diffraction patterns of the carbon supported catalysts was attributed to the (002) plane of the hexagonal structure of Vulcan XC-72R carbon black. There were no obvious peaks for Sn, Ni or their oxides; however their presence cannot be discounted. They might be present in small amounts or even transformed into an amorphous form. The calculated alloying degree of Sn in the PtSn (Table 2) observed the present of the amorphous form or Sn oxides in the catalysts. For bimetallic catalysts, only ca. 3-16% of Sn atoms were alloyed in the PtSn alloy formation. In addition, the commercial PtSn/C has higher alloyed of Sn about 40% in comparison to its home-made PtSn/C catalysts.

The (220) reflection of Pt was referred to estimate the average particle size according to

Table 1. The atomic compositions and metals loading of all catalysts (* determined by EDAX)

Catalysts	Atomic ratio *			All metals loading* (%)
	Pt	Sn	Ni	
Pt/C				20
Pt_3Sn_1/C	2.70	1.0	-	33.5
Pt_2Sn_1/C	1.95	1.0	-	19.4
Pt_1Sn_1/C	1.20	1.0	-	40.3
$Pt_4Sn_4Ni_1$/C	4.10	3.9	1.0	62.9

Table 2. The average particle sizes, $2\theta_{max}$ position, lattice parameter and alloying degree of all catalysts

Catalysts	Average particle size (nm)		$2\theta_{max}$ (°)	Lattice parameter (Å)	Alloying Degree (%)
	TEM	XRD			
Pt/C	3.0 ± 0.8	3.1	67.23	3.9355	-
Pt_3Sn_1/C	4.3 ± 1.4	3.9	67.14	3.9397	3.3
Pt_2Sn_1/C	4.7 ± 1.8	4.9	66.71	3.9627	10.9
Pt_1Sn_1/C	3.3 ± 0.8	2.6	66.67	3.9648	16.3
$Pt_4Sn_4Ni_1$/C	4.1 ± 1.4	3.4	68.29	3.8513	-

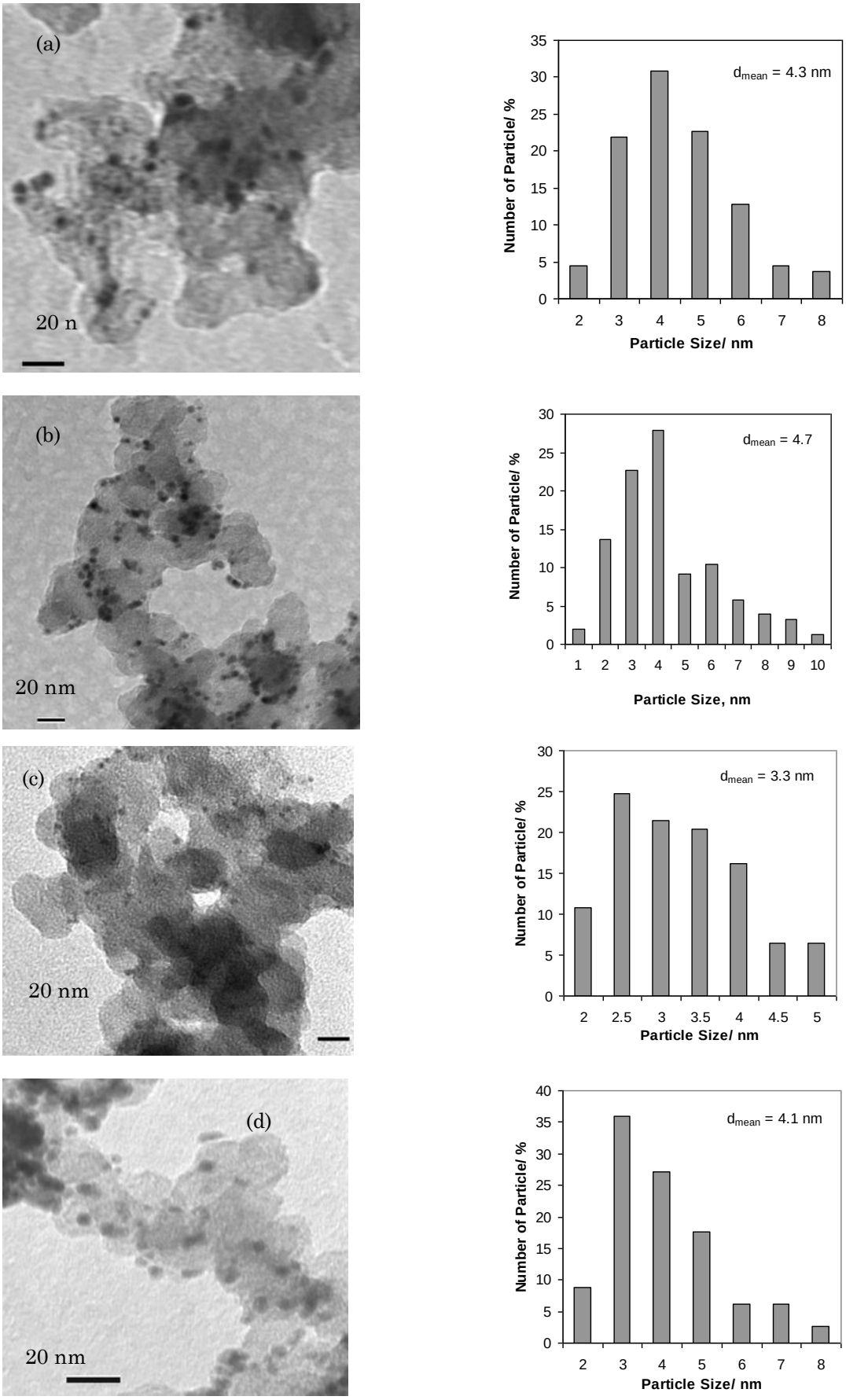

Figure 1. TEM images and histograms of catalysts: (a) Pt_3Sn_1/C, (b) Pt_2Sn_1/C, (c) Pt_1Sn_1/C, (d) $Pt_4Sn_4Ni_1/C$.

the Scherrer formula and lattice parameter [21]. The diffraction peak of Pt (220) was used as the reference to avoid possible disturbances from carbon black [22]. The average particle size and lattice parameter calculated from XRD patterns are summarised in Table 2. Calculated average particle sizes are in the range of 3-5 nm which are similar to those obtained using TEM measurement.

The XRD patterns reported in Figures 2 and 3, show remarkable differences between the carbon supported Pt and PtSn-based catalysts in their average particle sizes and the peak position of the (220) planes. The diffraction peak of the PtSn/C and PtSnNi/C catalysts shifted into opposite directions in comparison with Pt/C catalyst. In the case of PtSn/C catalysts, the addition of Sn to Pt increased the lattice parameter of the Pt (fcc) crystal structure as indicated by the shift to lower 2θ values in the (220) diffraction peaks. The shift might be attributed to alloy formation between Pt and Sn [23]. With increasing Sn content, there was a greater shift in lattice parameter away from pure Pt. These results were in agreement with recent data for PtSn/C catalysts using a borohydride reduction method [14]. The presence of Ni in Pt-Sn, on the contrary to Sn alone, shifted the diffraction peak to higher 2θ value. The shift is an indication of the reduction in the lattice parameter.

3.1. Electrochemical Characterisation

Figure 4 shows the cyclic voltamograms of carbon supported Pt and home-made electrocatalysts in the absence of ethanol at room temperature. All CVs reported after a stable and consistent scans were achieved. The scan rate was measured to be 5 mV s^{-1}. The current was normalised to mA per mg Pt loading. The coulombic charge of hydrogen adsorption region obtained after subtracting charge contributed from the double layer region was used to calculate specific electrochemical active surface areas (ESAH). The EASH data for all catalysts are summarised in Table 3. The Pt/C and Pt alloyed catalysts have similar active surface area, which were approximately 70-86 m^2 g^{-1} of Pt loading.

It shows that the CVs of PtSn electrocatalysts did not have a well-defined hydrogen region compared to that of pure Pt. As observed from the XRD result, platinum alloying by Sn or SnNi has altered the crystalline lattice parameter which may affect the adsorption and desorption of hydrogen. The Pt alloy generally exhibited larger current densities in the double layer region, which may be related to the presence of SnO_2 [23,24]. Furthermore, the voltammograms show that alloyed Pt catalysts assign the formation of oxygen-containing species through water adsorption starting at around 0.4 V. These potentials are much lower than that experienced on a Pt/C catalyst, i.e. at above 0.7 V [25].

CO stripping voltammetry was studied at a scan rate of 20 mV s^{-1} and in 0.5 mol dm^{-3} H_2SO_4

Table 3. The active surface area (ESA) of catalysts calculated from cyclic and CO stripping voltammograms

Catalysts	ESA_H (m^2 g^{-1}_{Pt})	ESA_{CO} (m^2 g^{-1}_{Pt})
Pt/C	77.9	67.3
Pt_3Sn_1/C	71.3	60.0
Pt_2Sn_1/C	84.0	64.4
Pt_1Sn_1/C	86.1	65.8
$Pt_4Sn_4Ni_1/C$	85.0	79.0

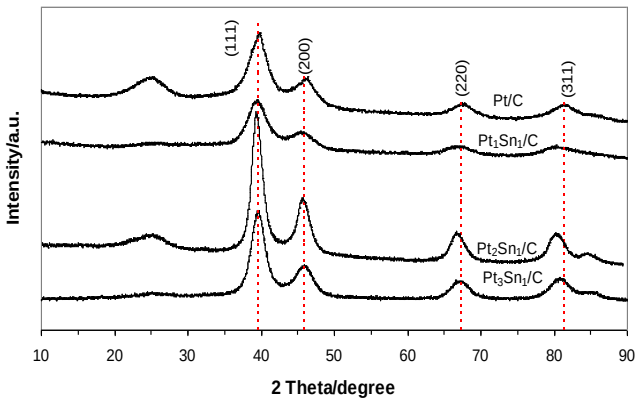

Figure 2. XRD patterns of Pt-Sn catalysts compared to Pt/C commercial catalyst

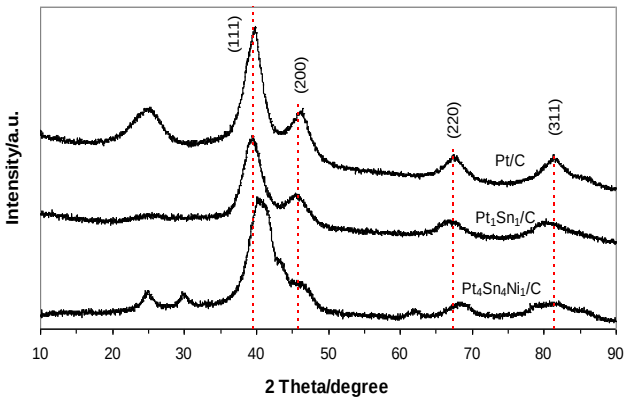

Figure 3. XRD patterns of ternary PtSnNi/C and Pt/C commercial catalysts

to estimate the active surface area (ESACO) of the alloyed Pt electro-catalysts and to obtain electrochemical information regarding the Pt-based catalysts surface. The ESACO of the electro-catalysts were calculated using Equation (1).

$$\mathrm{ESA_{CO}} = \frac{Q_{CO}}{420} \qquad (1)$$

where Q_{CO} is the charge of the CO desorption in micro coulomb normalised with the mass of Pt loading on the electrode, and 420 is the adsorption charge for a monolayer of CO on the catalyst in μC cm^{-2}.

The ESACO of the Pt-based electrocatalysts are given in Table 3, and their CO stripping voltammograms are presented in Figure 5. The ESACO (normalised by gram of Pt) increased with increasing Sn content in the PtSn alloy catalysts. The active area was observed to be around 60, 64 and 66 m^2 g^{-1} (Pt loading) for PtSn catalysts with atomic ratio of 3:1, 2:1 and 1:1, respectively. The Pt_1Sn_1/C catalyst with the highest Sn content exhibited the highest ESACO. This result, interestingly, has similar trend with the lattice parameter. The ESACO value and lattice parameter of Pt crystalline in PtSn catalysts increase as the Sn content increases.

The effect of the adsorbed CO on the catalysts surface was to remove the peak associated with hydrogen activity and to produce a CO oxidation peak in the first positive sweep. The CO oxidation has produced a sharp peak at around 0.8 V and the onset potential was ca. 0.7 V. The cyclic voltammogram for Pt/C catalyst, showed oxygenated species generated by water oxidation at above 0.7 V and carbon monoxide electro-oxidation on pure Pt catalyst consequently started at this point. Generally, alloyed Pt catalysts exhibited lower onset potentials for CO oxidation than pure platinum, i.e. around 0.4 V, as water oxidation occurred at the same value. Moreover, for bimetallic catalysts, the CO oxidation peak was broader as well as lower.

The shift of the CO oxidation onset potential to lower values for the alloyed PtSn/C compared to the Pt/C catalyst is in agreement with works reported previously [26-28]. The higher CO oxidation activity at lower potential on the alloyed Pt catalysts may be due to a more effective bifunctional mechanism at lower potential. The ability of Sn to promote the oxidation of adsorbed CO on the Pt sites was by adsorbing OH^- species produced from water disassociation [26,29,30] as described in Equation (2).

$$\mathrm{Pt\text{-}(CO)_{ad} + Sn\text{-}(OH)_{ad} \rightarrow Pt\text{-}Sn + CO_2 + H^+ + e^-} \qquad (2)$$

Other groups also reported that the Sn in alloys had an electronic effect, due to the Pt lattice expansion by incorporation of Sn atom [14,30,31]. The electronic or ligand effect may change the electronic properties of Pt sites as a consequence of the bonding between Pt and Sn. The expansion of Pt lattice parameter may cause a change in the charge transfer from Sn atoms to neighbouring Pt atoms and

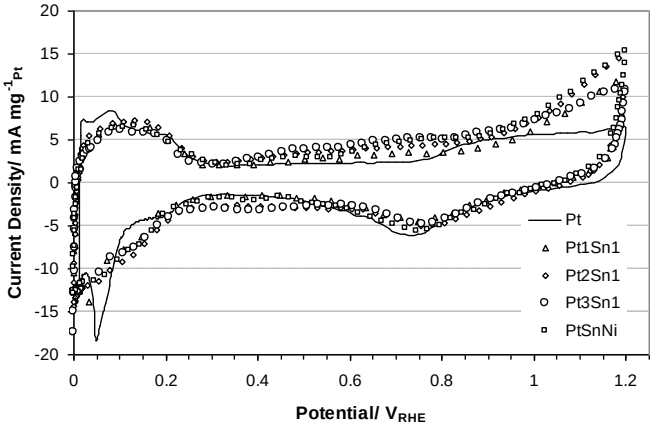

Figure 4. The cyclic voltammogram of the PtSn/C and Pt/C catalysts in 0.5 mol dm^{-3} of H_2SO_4 solution, at scan rate of 5 mV s^{-1} and 25 °C. (1) Pt/C, (2) Pt_1Sn_1/C, (3) Pt_2Sn_1/C, (4) Pt_3Sn_1/C, (5) $Pt_4Sn_4Ni_1/C$

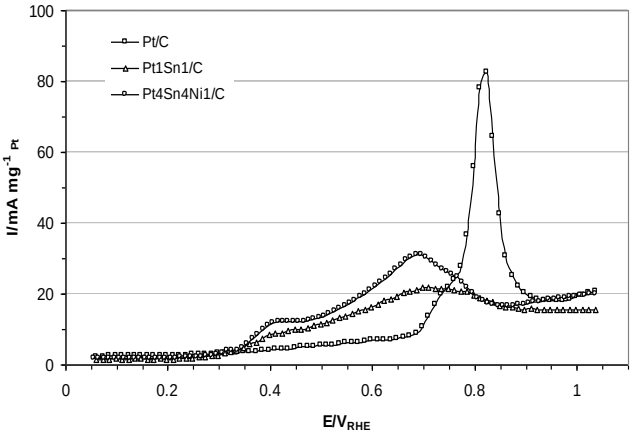

Figure 5. Voltammograms for CO electro-oxidation on Pt/C, Pt_1Sn_1/C and $Pt_4Sn_4Ni_1/C$ catalysts, 0.5 mol dm^{-3} H_2SO_4 at room temperature, 20 mV s^{-1} of scan rate

decrease in the Pt 4f binding energy. This electronic effect weakens adsorbed CO on the surface of Pt sites [14].

The presence of Ni in the PtSn catalyst increased slightly the active area from 66 to 79 m^2 g^{-1} (see Table 2) in which determined from the CO oxidation. From previous studies, Park *et al.* [32] reported that Ni shifted the Pt 4f binding energy for PtNi and PtRuNi to lower values than that for Pt. Electron transfer might contribute to enhance CO oxidation. Other research has reported that Ni enhanced PtRu catalyst during CO, methanol and ethanol oxidation [32, 33]. The Pt-Ni electronic interaction dominated the promoting effect of Ni on absorbed CO oxidation by weakening the Pt-CO bonding energy rather than the bifunctional mechanism.

The presence of a second or third metal added to Pt is necessary to improve catalytic activity for ethanol oxidation. Especially in an acid environment, Pt alone has limited ability to cleave the C-C bond and oxidize the adsorbed CO, which is considered to be disadvantages in ethanol oxidation [8]. Figures 6 and 7 show linear sweep voltammograms for the binary and ternary electro-catalysts for ethanol oxidation.

The electro-oxidation of ethanol on the Pt/C catalyst started at 0.45 V, whilst the addition Sn to Pt/C catalyst shifted the onset potentials to lower values (ca. 0.25-0.4 V). Interestingly, the Sn content significantly influenced the onset potential of ethanol electro-oxidation. The better electroactivity, i.e. lowest onset potential, was obtained for the PtSn/C catalysts with an atomic ratio of 1:1 (0.25 V), followed by those with ratios of 2:1 (0.27 V) and 3:1 (0.40 V), respectively. In comparison, the commercial PtSn/C showed the onset potential of 0.18 V recorded at a scan rate of 5 mV s^{-1} and the temperature of 30 °C. The present of alloyed PtSn or Sn oxides provide oxygenated species at lower potential. As soon as Sn-OH was formed, the adsorbed CO and other intermediates were oxidised which are called bifunctional mechanism. Due to its lower degree of alloying, Sn oxides may act mainly as an active sites at lower potential for dissociative adsorption of water.

Spinacé *et al.* [20] prepared catalysts with a similar method and results, whilst Lamy *et al.* [13] showed a superior ethanol electro-oxidation performance using PtSn/C catalyst electro-catalysts prepared by the Bönneman method, with atomic ratio of 9:1. With employing a thermal decomposition of a polymeric precursor, PtSn (60:40) gave the best activity for ethanol electro-oxidation for catalysts deposited on a Ti substrate [34]. Thus the preparation procedure strongly affects the electrocatalytic activity of PtSn/C catalysts for ethanol oxidation.

Figure 6 presents the LSV data for ethanol electro-oxidation on carbon supported PtSn and PtSnNi catalysts in acidic medium at temperature of 25 and 60 °C. In comparison to the Pt1Sn1/C catalyst, the addition of Ni to Pt-Sn did not change the onset potential of ethanol electro-oxidation, however enhanced the current density at a potential above 0.5 V. Similar results were obtained by Spinacé *et al.* [20] for PtSn/C and PtSnNi catalysts at room temperature with atomic ratios of 1:1 and 5:4:1, respectively. As reported that temperature did not alter the rds of ethanol electro-oxidation on all observed catalysts, even though it lowered the onset potential and in-

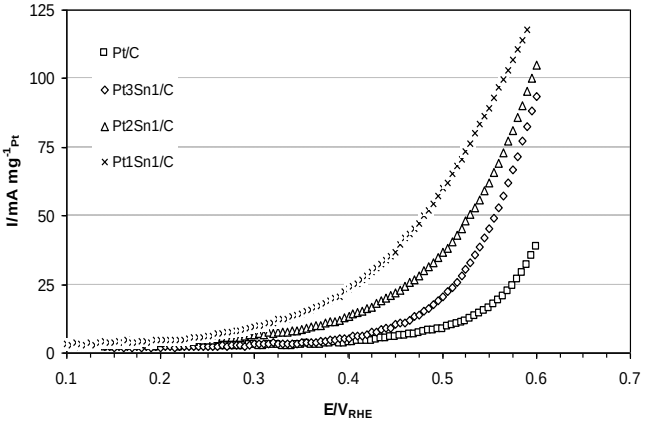

Figure 6. Linear sweep voltammograms of ethanol electro-oxidation on PtSn/C and Pt/C catalysts, 1 mol dm^{-3} ethanol and 0.5 mol dm^{-3} H_2SO_4 solution, scan rate of 2 mV s^{-1} at 25 °C.

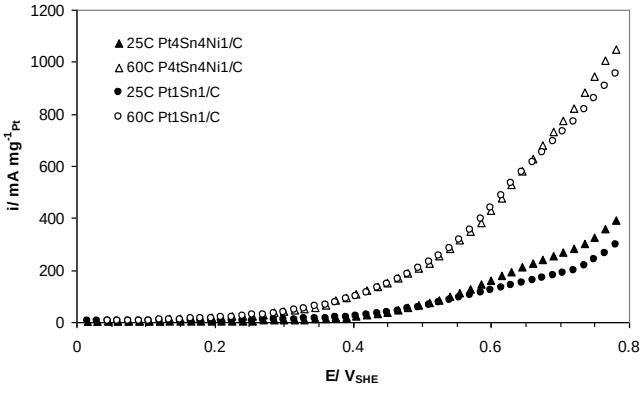

Figure 7. Linear sweep voltammograms of ethanol electro-oxidation on Pt_1Sn_1/C and $Pt_4Sn_4Ni_1/C$ catalysts. 1 mol dm^{-3} ethanol and 0.5 mol dm^{-3} H_2SO_4 solutions, scan rate of 2 mV s^{-1} at 25 and 60 °C

creased mass activity, i.e. current density. Therefore, the effect of temperature in detail was not further investigated.

As discussed previously, the presence of Ni in the PtSn catalyst enhanced CO oxidation by weakening Pt-CO bond (ligand effect). When Pt site was able to provide the OH species at a high potential (>0.5 V), it was noticed that the weaker adsorbed CO was oxidised easily. An increased active area also contributed to provide wider catalyst surface in order to adsorb ethanol.

The current density of ethanol electro-oxidation on PtSn/C at 0.55 V and temperature of 25 ^{o}C was about 89 mA mg^{-1}, whilst that of on PtSnNi/C was about 10 mA mg^{-1} higher. At temperature of 60 ^{o}C, the current density of ethanol electro-oxidation on PtSnNi/C was about 40 mA mg^{-1} higher than that of on PtSn/C at 0.7 V.

The corresponding Tafel plots are shown in Figure 8 and a further comparison of ethanol electro-oxidation activity is shown in the chrono-amperometry data (Figure 9). Each measurement was performed over 5 minutes to approach steady state conditions. It can be seen that the current density of ethanol electro-oxidation on $Pt_4Sn_4Ni_1$/C catalyst was slightly higher than that for Pt_1Sn_1/C catalyst; in agreement with the LSV data. The current densities were found to be 13 and 15 mA mg^{-1} Pt for Pt_1Sn_1/C and $Pt_4Sn_4Ni_1$/C at 0.4 V. Whilst the ethanol electro-oxidation current density on $Pt_4Sn_4Ni_1$/C was measured to be 9 and 62 mA mg^{-1} Pt at 0.5 and 0.6 V, respectively.

Kinetic parameters were determined from Tafel plots obtained from LSV and chronoamperometry data. Tafel slopes and exchange current densities for all catalysts are listed in Table 4. Tafel slopes for Pt_1Sn_1/C and $Pt_4Sn_4Ni_1$/C catalysts were found to be similar at around 90-100 mV dec^{-1}, whilst those for Pt_2Sn_1/C, Pt_3Sn_1/C and Pt/C catalysts were 85, 72 and 55 mV dec^{-1}, respectively. The close Tafel slope values of PtSn/C catalysts indicate a similar mechanism of ethanol electro-oxidation on those catalysts.

However, the Tafel slope of catalyst with high Sn loading (Pt_1Sn_1/C) is quite far with that of Pt/C, thus the rds may change. The difference in Tafel slopes should be related to the number of electron associated with the overall reaction. As mentioned previously, ethanol electro-oxidation on Pt or Pt alloyed catalysts included several complex reactions. The adsorption of ethanol occurs on Pt, whereas alloyed metals such Sn most likely offer OH- adsorption at lower potential to remove the adsorbed CO or to convert the intermediate into acetic acid. The mean electron number of 2 and 4 correspond mainly to the ethanol electro-oxidation into acetaldehyde and acetic acid formation, respectively. Rousseou and coworker [35] investigated product distribution in DEFCs test with different anode catalysts, i.e. Pt/C, PtSn/C and PtSnRu/C. The addition of Sn to Pt favoured the formation acetic acid over acetaldehyde, in comparison to the pure Pt, but the yield of CO_2 was detected to be doubled with a Pt/C than with a PtSn/C catalyst. Those results are in agreement with Ta-

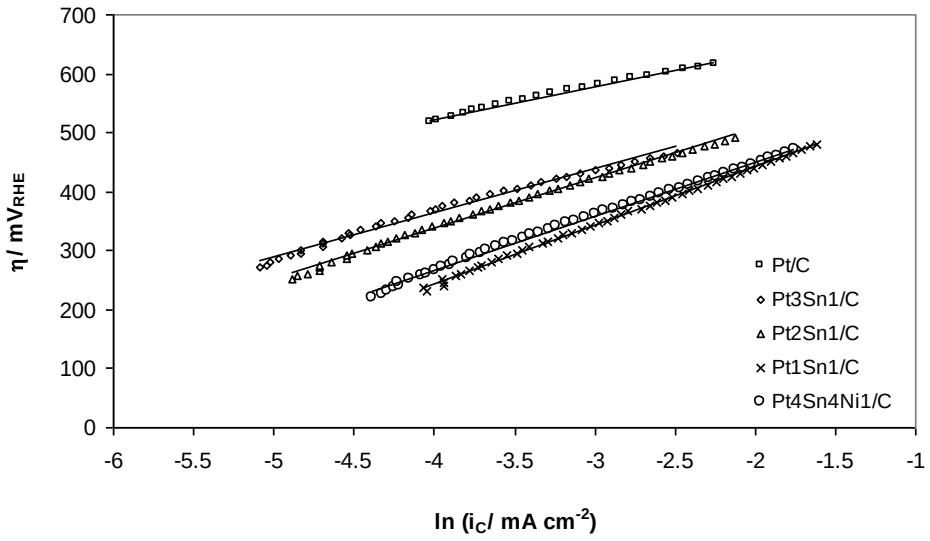

Figure 8. Tafel plots of ethanol electro-oxidation on PtSnNi/C, PtSn/C and Pt/C catalysts in 1 mol dm^{-3} ethanol and 0.5 mol dm^{-3} H_2SO_4 solution. The current density was normalised to the active surface area (ESA_{CO}) of the respective catalysts

fel slopes that are obtained from this work for a high loading Sn catalyst. The Pt/C catalyst shows having the lowest slope which indicates that the overall reaction on Pt/C has generated more electrons in comparison to that on Pt alloyed catalysts. Hence, the selectivity towards the formation of acetic acid, acetaldehyde and CO_2 correlate to the number of electron generated by the total reaction and rate determining step in the mechanism reaction.

Exchange current densities of Pt/C, Pt_3Sn_1/C Pt_2Sn_1/C Pt_1Sn_1/C and Pt_4Sn_4Ni/C were about 1.3×10^{-6}, 1.1×10^{-4}, 3.5×10^{-4}, 1.5×10^{-3}, and 1.0×10^{-3} mA cm^{-2}, respectively. Those values were normalised by the active surface area (ESACO). Exchange current densities for PtSn catalysts increase with the increase of Sn content. In this work, the highest exchange current density was obtained for the Pt_1Sn_1/C catalyst. This reflects the rate of ethanol electrooxidation on the surface of PtSn/C catalyst is faster than that on others. However, the addition of Ni to PtSn slightly reduces the exchange current density. Zhu *et al.* [36] reported the exchange current densities of PtSn/C catalysts of 5.38, 2.52 and 0.102 mA cm^{-2} prepared with different methods that were obtained from anode polarisation curve at 90 ^oC for PtSn/C-B, PtSn/C-EG and $PtSnO_2$/C, respectively. Exchange current densities were however based on the cross-section of the electrode. The PtSn/C-B which had the highest alloying degree displayed enhancement of activity for ethanol electro-oxidation.

4. Conclusions

Carbon supported PtSn with different atomic ratio and PtSnNi were prepared by a polyol method. Nano-particles with diameters between 2.5-5.0 nm were obtained. According to the XRD results, the peak of (220) crystalline face centred cubic (fcc) Pt phase for PtSn and PtSnNi alloys was repositioned due to the presence of Sn and/or Ni in the alloy. The modification of structural and electronic features was observed as the shift of lattice parameter might facilitate a better adsorbed CO oxidation. Furthermore, the modification of Pt with Sn and SnNi improved ethanol and CO electro-oxidation. According to the bifunctional mechanism, the present of Sn oxides provided oxygenated species at lower potentials in comparison to pure Pt. The observed

Table 4. Tafel slope and exchange current density values of all catalysts

Catalysts	Tafel slopes (mV dec^{-1})	Exchange current densities (mA cm^{-2})
Pt/C	55	$1.3\ 10^{-6}$
Pt_3Sn_1/C	72	$1.1\ 10^{-4}$
Pt_2Sn_1/C	85	$3.5\ 10^{-4}$
Pt_1Sn_1/C	99	$1.5\ 10^{-3}$
$Pt_4Sn_4Ni_1$/C	92	$1.0\ 10^{-3}$

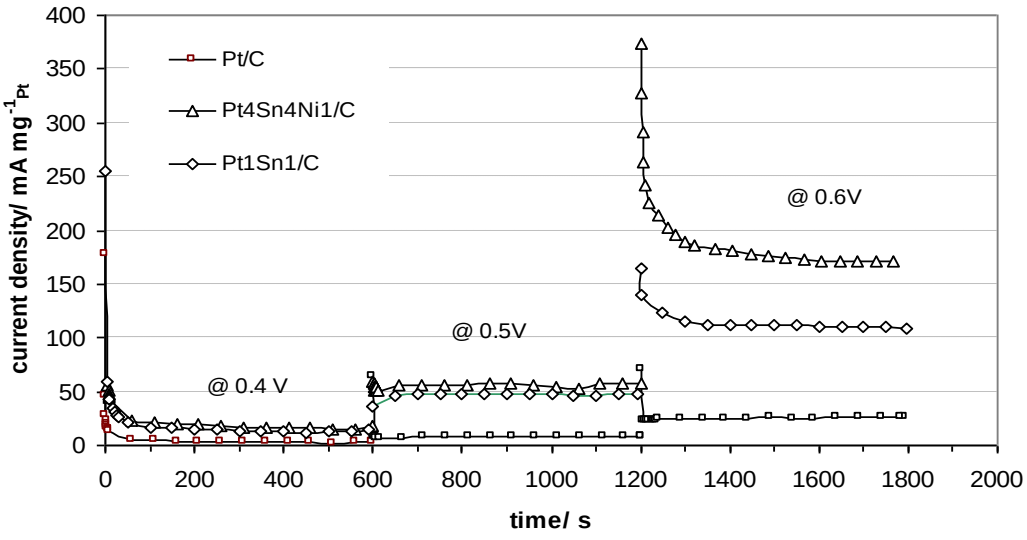

Figure 9. Chronoamperometric curves of ethanol electro-oxidation for Pt_1Sn_1/C and $Pt_4Sn_4Ni_1$/C catalysts. 1 mol dm^{-3} ethanol and 0.5 mol dm^{-3} H_2SO_4 at room temperature

Tafel slopes suggested that bi and tri-metallic Pt-based catalysts with high Sn loading have altered the rate determining step of mechanism which the overall reaction on those catalysts produced fewer electrons than that on pure Pt. However, the exchange current density of ethanol oxidation reaction on Pt-based catalysts was accelerated significantly by factor of 100-1000. In general, PtSnNi/C catalysts showed a better electrocatalytic activity than PtSn/C catalysts in half-cell tests.

Acknowledgments

This work was performed with scholarship support from Schlumberger Foundation with the program of Faculty for the Future.

References

[1] Lamy, C., Belgsir, E.M., Léger, J.M. (2001). Electrocatalytic oxidation of aliphatic alcohols: Application to the direct alcohol fuel cell (DAFC). *J. Appl. Electrochem.*, 31: 799-809.

[2] Zhou, W., Zhou, Z., Song S, Li. W., Sun, G., Tsiakaras, P., Xin, Q. (2003). Pt based anode catalysts for direct ethanol fuel cells. *Appl. Catal. B. Environ.*, 46: 273-285.

[3] Delime, F., Leger, J.M., Lamy, C. (1999). Enhancement of the electrooxidation of ethanol on a Pt-PEM electrode modified by tin. Part I: Half cell study. *J Appl Electrochem*, 29: 1249-1254.

[4] Camara, G., de Lima, R., Iwasita, T. (2004). Catalysis of ethanol electrooxidation by PtRu: the influence of catalyst composition. *Electrochem. Commun.,* 6: 812-815.

[5] Liu, Z., Ling, X.Y., Su, X., Lee, J.Y., Gan, L.M. (2005). Preparation and characterization of Pt/C and PtRu/C electrocatalysts for direct ethanol fuel cells. *J. Power Sources,* 149: 1-7.

[6] Mann, J., Yao, N., Bocarsly, A.B. (2006). Characterization and analysis of new catalysts for a direct ethanol fuel cell. *Langmuir*, 22: 10432-10436.

[7] Sen Gupta, S., Datta, J.A. (2006). Comparative study on ethanol oxidation behavior at Pt and PtRh electrodeposits. *J. Electroanal. Chem*, 594: 65-72.

[8] Zhou, W.J., Li, W.Z., Song, S.Q., Zhou, Z.H., Jiang, L.H., Sun, G.Q., et al. (2004). Bi- and tri-metallic Pt-based anode catalysts for direct ethanol fuel cells. *J .Power Sources*, 131: 217-223.

[9] Song, S.Q., Zhou, W.J., Zhou, Z.H., Jiang, LH., Sun, G.Q., Xin, Q., et al. (2005). Direct ethanol PEM fuel cells: The case of platinum based anodes. *Int. J. Hydrogen Energy*, 30: 995-1001.

[10] Wang, H., Jusys, Z., Behm, R.J. (2006). Ethanol electro-oxidation on carbon-supported Pt, PtRu and Pt_3Sn catalysts: A quantitative DEMS study. *J. Power Sources,* 154: 351-359.

[11] Jiang, L., Colmenares, L., Jusys, Z., Sun, G.Q., Behm, R.J. (2007). Ethanol electrooxidation on novel carbon supported Pt/SnOx/C catalysts with varied Pt:Sn ratio. *Electrochim. Acta,* 53: 377-389.

[12] Guo, Y., Zheng, Y., Huang, M., (2008). Enhanced activity of PtSn/C anodic electrocatalyst prepared by formic acid reduction for direct ethanol fuel cells. *Electrochim. Acta,* 53: 3102-3108.

[13] Lamy, C., Rousseau, S., Belgsir, E.M., Coutanceau, C., Léger, J.M. (2004). Recent progress in the direct ethanol fuel cell: Development of new platinum-tin electrocatalysts. *Electrochim. Acta,* 49: 3901-3908.

[14] Kim, J.H., Choi, S.M., Nam, S.H., Seo, M,H., Choi, S.H., Kim, W.B. (2008). Influence of Sn content on PtSn/C catalysts for electrooxidation of C_1-C_3 alcohols: Synthesis, characterization, and electrocatalytic activity. *Appl. Catal. B Environ.*, 82: 89-102.

[15] Colmati, F., Antolini, E., Gonzalez, E.R. (2007). Ethanol Oxidation on Carbon Supported Pt-Sn Electrocatalysts Prepared by Reduction with Formic Acid. *J. Electrochem. Soc.,* 154: B39-B47.

[16] Zhou, W.J., Song, S.Q., Li, W.Z., Zhou, Z.H., Sun, G.Q., Xin, Q., et al. (2005). Direct ethanol fuel cells based on PtSn anodes: the effect of Sn content on the fuel cell performance. *J. Power Sources*. 140: 50-58.

[17] Vigier, F., Coutanceau, C., Hahn, F., Belgsir, E.M., Lamy, C. (2004). On the mechanism of ethanol electro-oxidation on Pt and PtSn catalysts: Electrochemical and in situ IR reflectance spectroscopy studies. *J. Electroanal. Chem*. 63: 81-89..

[18] Jiang, L., Sun, G., Zhou, Z., Zhou, W., Xin, Q. (2004). Preparation and characterization of PtSn/C anode electrocatalysts for direct ethanol fuel cell. *Catal. Today*, 93-95: 665-670.

[19] Jiang, L., Sun, G., Sun, S., Liu, J., Tang, S., Li, H, et al. (2005). Structure and chemical composition of supported Pt–Sn electrocatalysts for ethanol oxidation. *Electrochim. Acta* , 50: 5384-5389.

[20] Spinacé, E. V., Linardi, M., Neto, A.O.(2005). Co-catalytic effect of nickel in the electro-oxidation of ethanol on binary

Pt–Sn electrocatalysts. *Electrochem. Commun.*, 7: 365-369.

[21] Eberhart, J. (1991). *Structural and Chemical Analysis of Materials: X-ray, Electron and Neutron Diffraction, X-ray, Electron and Ion Spectrometry, Electron Microscopy*. John Wiley and Sons Ltd.

[22] Mukerjee, S., Srinivasan, S., Soriaga, M.P., McBreen, J. (1995). Role of structural and electronic properties of Pt and Pt alloys on electrocatalysis of oxygen reduction. An in situ XANES and EXAFS investigation. *J Electrochem. Soc.*, 142: 1409-1422.

[23] Colmati, F., Antolini, E., Gonzalez, E.R. (2007). Ethanol oxidation on a carbon-supported $Pt_{75}Sn_{25}$ electrocatalyst prepared by reduction with formic acid: Effect of thermal treatment. *Appl. Catal. B Environ.*, 73: 106-115.

[24] Spinacé, E., Neto, A., Linardi, M. (2004). Electro-oxidation of methanol and ethanol using PtRu/C electrocatalysts prepared by spontaneous deposition of platinum on carbon-supported ruthenium nanoparticles. *J. Power Sources,* 129: 121-126.

[25] Lim, D-H., Choi, D-H., Lee, W-D., Park, D-R., Lee, H-I. (2007) The Effect of Sn Addition on a Pt/C Electrocatalyst Synthesized by Borohydride Reduction and Hydrothermal Treatment for a Low-Temperature Fuel Cell. *Electrochem, Solid-State Lett.*, 10: B87–B90.

[26] Arenz, M., Stamenkovic, V., Blizanac, B., Mayrhofer, K, Markovic, N., Ross, P. (2005) Carbon-supported Pt–Sn electrocatalysts for the anodic oxidation of H_2, CO, and H_2/CO mixtures.Part II: The structure-activity relationship. *J. Catal.*, 232: 402-410.

[27] Lim, D-H., Choi, D-H., Lee, W-D., Lee, H-I. (2009) A new synthesis of a highly dispersed and CO tolerant PtSn/C electrocatalyst for low-temperature fuel cell; its electrocatalytic activity and long-term durability. *Appl. Catal. B Environ.*, 89: 484-493.

[28] Colmenares, L., Wang, H., Jusys, Z., Jiang, L., Yan, S., Sun, G.Q., *et al.* (2006). Ethanol oxidation on novel, carbon supported Pt alloy catalysts - Model studies under defined diffusion conditions. *Electrochim. Acta*, 52: 221-233.

[29] Hayden, B.E., Rendall, M.E., South, O. (2005). The stability and electro-oxidation of carbon monoxide on model electrocatalysts: Pt(111)–Sn(2×2) and Pt(111)–Sn($\sqrt{3}\times\sqrt{3}$)R30°. *J. Mol. Catal. A Chem.*, 228: 55-65.

[30] Gasteiger, H.A., Marković, N.M., Ross, P.N. (1996). Structural effects in electrocatalysis: electrooxidation of carbon monoxide on Pt3Sn single-crystal alloy surfaces. *Catal. Letters*, 36: 1-8.

[31] Tripković, A.V., Popović, K.D., Lović, J.D., Jovanović, V.M., Stevanović, S.I., Tripković, D.V., *et al.* (2009). Promotional effect of Snad on the ethanol oxidation at Pt_3Sn/C catalyst. *Electrochem. Commun.*, 11: 1030-1033.

[32] Martínez-Huerta, M.V., Rojas, S, Gómez, D. L., Fuente, J.L, Terreros, P, Peña, M.A., Fierro, J.L.G. (2006). Effect of Ni addition over PtRu/C based electrocatalysts for fuel cell applications. *Appl. Catal. B Environ.*, 69: 75-84.

[33] Wang, Z-B., Yin, G-P., Zhang, J., Sun, Y-C., Shi, P-F. (2006). Investigation of ethanol electrooxidation on a Pt-Ru-Ni/C catalyst for a direct ethanol fuel cell. *J. Power Sources*, 160: 37-43.

[34] Simões, F.C., dos Anjos, D.M., Vigier, F., Léger, J-M., Hahn, F., Coutanceau, C., et al. (2007). Electroactivity of tin modified platinum electrodes for ethanol electrooxidation. *J. Power Sources*, 167: 1-10.

[35] Rousseau, S., Coutanceau, C., Lamy, C., Léger, J-M. (2006). Direct ethanol fuel cell (DEFC): Electrical performances and reaction products distribution under operating conditions with different platinum-based anodes. *J. Power Sources*, 158: 18-24.

[36] Zhu, M., Sun, G., Xin, Q. (2009). Effect of alloying degree in PtSn catalyst on the catalytic behavior for ethanol electro-oxidation. *Electrochim. Acta*, 54: 1511-1518.

Selected and Revised Papers from The 2nd International Conference on Chemical and Material Engineering 2015 (ICCME 2015) (29-20 September, 2015, Semarang, Indonesia) (http://econference.undip.ac.id/index.php/iccme/2015) after Peer-reviewed by ICCME 2015 and BCREC Reviewers